Available online at website: https://journal.bcrec.id/index.php/bcrec

Bulletin of Chemical Reaction Engineering & Catalysis, 19 (1) 2024, 149-159

Research Article

Hexagonal TiO_2/SiO_2 Porous Microplates for Methylene Blue Photodegradation

Maria Ulfa[1,*], Cindy Nur Anggreani[1], Bakti Mulyani[1], Novia Amalia Sholeha[2]

[1]Chemistry Education Study Program, Faculty of Teacher Training and Education, Sebelas Maret University, Jl. Ir. Sutami 36A, Surakarta 57126, Indonesia.
[2]College of Vocational Studies, Bogor Agricultural University (IPB University), Jalan Kumbang No. 14, Bogor 16151, Indonesia.

Received: 17th January 2024; Revised: 17th February 2024; Accepted: 18th February 2024
Available online: 24th February 2024; Published regularly: April 2024

Abstract

Hexagonal TiO_2/SiO_2 Porous Microplates have been successfully synthesized by incorporation of Ti precursors into SiO_2 synthesized from Si precursors in a gelatin-CTAB mixture via the hydrothermal method. The prepared samples were characterized by X-ray diffraction (XRD), scanning electron microscopy (SEM), EDX, nitrogen adsorption-desorption and Fourier transform infrared spectroscopy (FTIR). The sample has a surface area of 735 m^2/g, pore volume of 0.67 cc/g, and pore diameter of 3.2 nm, according to the results of the characterization of hexagonal TiO_2/SiO_2 porous microplates. The transformation of SiO_2 microspheres into hexagonal TiO_2/SiO_2 porous microplates is revealed by a microparticle size increase of 84% and the transition of Si−O bonds into Ti−O and Si−O as measured by FTIR. The photocatalytic activity of hexagonal TiO_2/SiO_2 porous microplates resulted in 81.15% photodegradation of methylene blue under UV light irradiation within 60 min, which was 21 % better than SiO_2.

Keywords: hexagonal; microplates TiO_2/SiO_2; methylene blue; photodegradation

How to Cite: M. Ulfa, C.N. Anggreani, B. Mulyani, N.A. Sholeha (2024). Hexagonal TiO_2/SiO_2 Porous Microplates for Methylene Blue Photodegradation. *Bulletin of Chemical Reaction Engineering & Catalysis*, 19 (1), 149-159 (doi: 10.9767/bcrec.20120)

Permalink/DOI: https://doi.org/10.9767/bcrec.20120

1. Introduction

The increase of carcinogenic organic dye compounds, such as methylene blue, which are detrimental to human health, aquatic and non-aquatic organisms is boosting the growth of textile industry waste [1,2]. For the treatment of methylene blue waste by the formation of reactive chemical species, semiconductor-based photocatalyst materials were developed because they are environmentally acceptable, energy efficient, and tolerate mild reaction conditions without secondary contamination [3,4]. Under light irradiation, semiconductor photocatalysts such as titanium dioxide (TiO_2) [4,5], zinc oxide (ZnO) [6,7], copper oxide (CuO) [8,9] and cerium oxide (CeO_2) [10,11] have been employed extensively for the degradation of dyes such as methylene blue. TiO_2 has been widely utilized as a low-cost photocatalyst for the degradation of methylene blue in water due to its high electron mobility [12,13], long carrier life [14], chemical stability [15], wide radiation absorption range [16], high photosensitivity [17], and non-toxicity [18]. TiO_2 with a band gap energy of 3.3 eV at 300 K is common in the earth's crust and acts as a photocatalyst when exposed to ultraviolet light [19].

Tuning the photocatalytic performance of a TiO_2 structure by adjusting its size, shape, surface area, defect concentration, and exposed crystalline sites [20]. In addition, TiO_2 is photocatalytic because OH^- ions can preferentially adsorb on its positively charged surface, resulting in a higher generation rate of •OH radicals and enhanced photodegradation

* Corresponding Author.
Email: ulfa.maria2015@gmail.com
mariaulfa@staff.uns.ac.id (M. Ulfa)

[21]. Nevertheless, the possibility for TiO_2 agglomeration is strong enough to necessitate material support for particle dispersion [22]. SiO_2 is one of the materials that has a substantial impact as a catalyst support material. Numerous researchers have researched the synthesis of SiO_2 by various methods, but the topic of high-sustainability green precursors derived from natural materials has assumed a prominent role in the last ten years [23]. Gelatin is a naturally occurring substance with a high level of durability that has been utilized in several research to synthesize diverse morphologies of porous materials [24]. However, no study has yet been undertaken on coupling gelatin with other templates to create SiO_2 that is subsequently combined with Ti precursor.

In this study, hexagonal TiO_2/SiO_2 porous microplates were produced by incorporating titanium tetraisopropoxide (TTiP) as a Ti precursor onto SiO_2 microspheres as a supporting material. These microspheres were synthesized using the hydrothermal method in a solution containing gelatin and cetyltrimethylammonium bromide (CTAB). This work examined the alteration of shape, porosity, and photocatalytic activity for the degradation of methylene blue from SiO_2 to TiO_2/SiO_2 under UV light irradiation.

2. Material and Methods

2.1 Material

The materials used in this study were hydrochloric acid (HCl 37%, Sigma-Aldrich Merck KGa, MW = 36.5 g/mol), aquades (Smart-Lab, MW 18 g/mol), cetyltrimethylammonium bromide (CTAB, Sigma-Aldrich Merck KgaA, MW = 364.45 g/mol), commercial gelatine (Gelita, MW 90,000 g/mol), tetraethyl orthosilicate (TEOS, Sigma-Aldrich Merck KgaA, MW = 208.33 g/mol), titanium tetraisopropoxide (TtiP, Sigma-Aldrich Merck KgaA, MW = 204 g/mol), ethanol (Sigma-Aldrich Merck KgaA, MW = 46.068 g/mol), sodium hydroxide (NaOH, 99.8%, pellet, Sigma-Aldrich Merck KgaA, MW = 39.997 g/mol), and methylene blue (Sigma-Aldrich Merck KgaA, MW = 319.85 g/mol).

2.2 Synthesis of SiO_2 Microspheres

First, CTAB and gelatin are mixed with NaOH in water with a molar ratio of gelatin: CTAB : NaOH : water : TEOS = 6.6×10^{-5} : 0.27 : 0.087 : 26 : 0.02. The mixture was stirred at 80 °C for 2 h to form a white slurry. The resulting mixture was filtered, washed, and then dried at 70 °C for 24 h. The dried sol id was then calcified at 550 °C for 5 h at a rate of 2 °C/min to remove any residual surfactant. The results of the synthesis are labeled as SiO_2 microspheres (SM).

2.3 Synthesis of Hexagonal TiO_2/SiO_2 Porous Microplates (HTSMP)

First TEOT in hexane (1:800 v/v) is mixed in 1 gram of SiO_2 microsphere while stirring at 45 °C for 16 h. The mixture was then dried at 160 °C for 2 h and calcined annealed at 550 °C for 5 h. The results of the synthesis are labeled as hexagonal TiO_2/SiO_2 porous microplates (HTSMP).

2.4 Characterizations of the Material

The instrument used to test the sample included the Pan Analytical brand X-Ray Diffraction (XRD) (Version PW3050/60). From the diffractogram, crystal size is calculated by the Debye Scherrer formula as in the equation below of Equation (1).

$$D = \frac{0.9\lambda}{B\cos\theta} \tag{1}$$

where, D is the crystal size in Å, λ is the wavelength used in the XRD test, which is 1.54056 Å, and B is the width of half the peak in radians. θ is the angular position of the peak formation. XRD results also show FWHM to be able to determine the value of B (rad). The crystallinity of the sample can also be calculated through the X-Ray Diffraction characterization data using Equation (2).

$$Crystallinity = \frac{crystalline\ peak\ area}{crystalline\ and\ amorphous\ peak\ areas}\times100\% \tag{2}$$

The Shimadzu 21 brand Fourier Transform Infrared (FTIR) spectrophotometer with 0.5 cm^{-1} resolution, Scanning Electron Microscopy-Energy Dispersive X-Ray (SEM-EDX) with images taken with a JEOL JSM-700 microscope at a voltage speed of 15.0 kV, and Brunauer - Emmett-Teller (BET) brand Quantacrome Nova 1200e. a tool for testing samples using a Shimadzu UV-3600 Ultraviolet Visible (UV-Vis) Spectrophotometer with a wavelength of 665 nm.

2.5 Photodegradation of Methylene Blue

200 mL of 5 mg/L methylene blue solution plus 50 mg of photocatalyst. The photocatalyst process begins with 30 min of dark adsorption beneath a dark-closed shaker reactor. UV light irradiation then follows. Using a UV-Vis spectrophotometer with a wavelength range of 670 nm, the absorbance of 5 ml of solution was measured every 10 min by Equations (3)-(5).

$$\%ED = \frac{C_0 - C_t}{C_0}\times100\% \tag{3}$$

$$C_0 - C_t = kt \tag{4}$$

$$\ln \frac{C_0}{C_t} = -kt \quad (5)$$

where, %*ED* = Photodegradation efficiency of MB, C_0 = initial concentration of MB, C_t = concentration of MB at t minutes.

3. Results and Discussion

Figure 1 demonstrates that all samples exhibit an amorphous SiO_2 phase as indicated by the broad diffraction peak centered at 2θ = 23.08° according to the JCPDS file. 29-0085 [25]. Hexagonal TiO_2/SiO_2 porous microplates revealed that not only the SiO_2 peak but also the low TiO_2 peak at 2θ =25.5° were in good agreement with the JCPDS card number JCPDS No. 21-1276 as anatase [26]. Except for the successful identification of the amorphous SiO_2 phase in both samples, no significant changes were identified.

The existence of differences in composition before and after Ti impregnation apart from XRD can also be proven from EDX data. The SM has a percentage content of 72.69% Si, 25.15% O, and 2.16% C, but the composition changes after impregnation, i.e. 46.40% Si, 51.07% O, 2.14% C, and 0.32% Ti. The XRD data is strengthened by EDX data which shows that there is Ti content in mesoporous silica, which shows that the Ti impregnation process into Mesoporous Silica has been successfully carried out. Another phenomenon shows a decrease in the amount of Si after impregnation due to some of the Si in the framework being replaced by TiO_2 which is explained by the appearance of the Ti content and an increase in the amount of oxygen. Meanwhile, the amount of carbon tends to be stable, which indicates that there is a number of carbons from gelatin that bond strongly to silica during synthesis to form C–Si bonds through the strong affinity between –HC–NH_3 gelatin and Si–OH to bulid formation NH_3–HC-------Si–OH from silica precursors. C–Si bonds are formed after calcination at 550 °C due to insufficient heat energy to decompose all the carbon. This also illustrates that TiO_2 impregnation on mesoporous silica only blocks the silica surface as the dominant surface and has no effect on the carbon component.

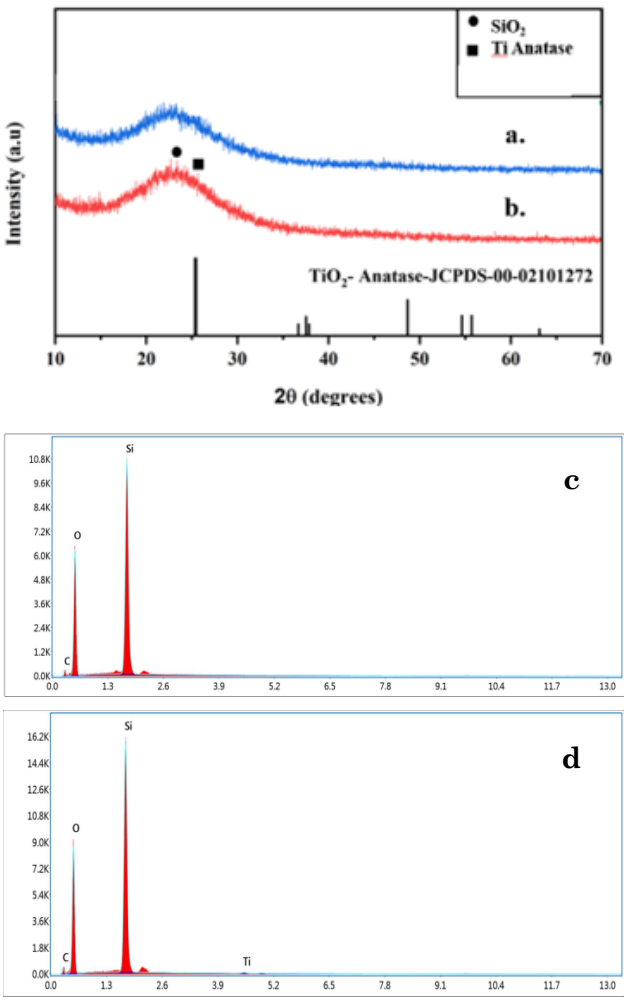

Figure 1. XRD diffactogram and EDX elemental mapping of (a,c) SiO_2 microspheres (b,d) Hexagonal TiO_2/SiO_2 Porous Microplates.

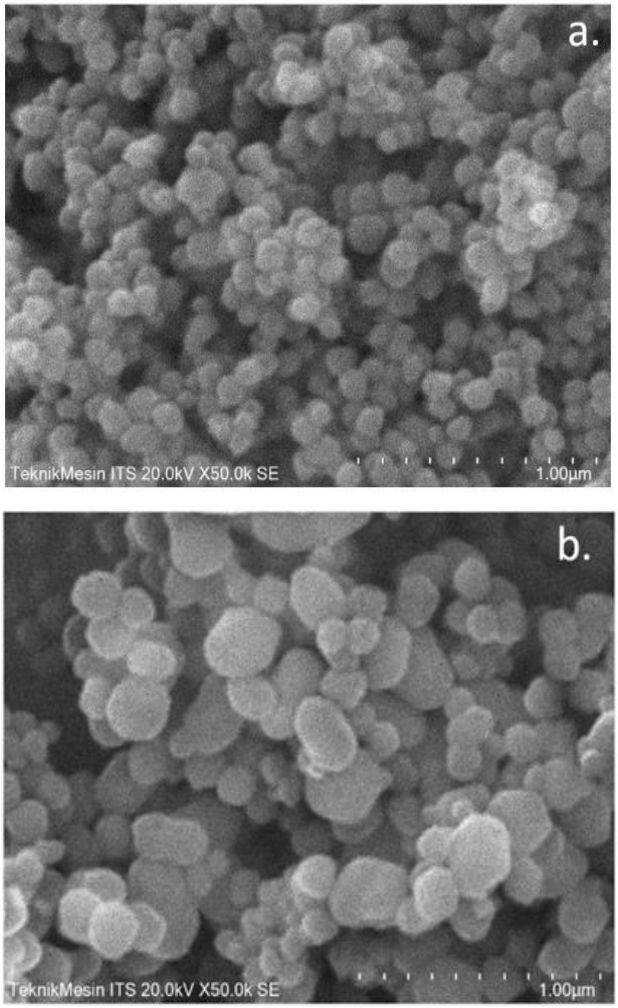

Figure 2. SEM image of a) SiO_2 microspheres (SM) and b) Hexagonal TiO_2/SiO_2 Porous Microplates (HTSMP).

Figure 2 illustrates the morphology of micro-sized SiO_2 microspheres and hexagonal TiO_2/SiO_2 porous microplates (HTSMP), respectively. This modification of the particle shape is predicted due to the employment of the sol-gel process in which there are two primary steps, namely hydrolysis and polycondensation [27]. In the CTAB hydrolysis stage, gelatin and NaOH produce a sol in the form of micro-sized particles suspended in the solution. The subsequent step is the gel, which is the polycondensation reaction in the form of a transition from the sol to a gel, during which the micro solids begin to condense into a more complicated network [28]. In the polycondensation stage, the interaction of CTAB, gelatin and alkaline solution drives droplet size so that the gel formed is a collection of semi-solid microdroplets. As a crystal core embryo, the microdroplet will undergo reorganization to form a larger and more regular agglomeration arrangement. The equilibrium between the crystal core embryo, the amorphous gel, and the remaining silica supply permits the expansion of the crystal nucleus into larger particles, which will continue to occur until the residual is depleted and crystals form in a stable condition, generating 0.19 µm silica microspheres.

Figure 2 also show that there are some particles that imperfect as hexagonal-like because the amount of Ti impregnated is small so the attraction between Ti–O–Si forming a hexagonal is also minimal. This small Ti give strong impact to form perfect hexagonal part by good interaction between silica and the Ti precursor during impregnation process. The part that does not interact with Ti is due to the minimal amount of Ti dispersed on the surface so nothing center electrostatic force to direct the hexagonal structure but Ti attraction only causes elongation and enlargement of the size of the silica on various surfaces . The result on the absence of interaction stimulants is stable spherical silica shape due to as previous research explnataion [29–31].

After incorporating Ti precursors into the surface of SiO_2 microspheres in hexane solvent, an unexpected result was discovered. When reacting with Ti precursor in hexane, the Si–OH surface of silica produces a high electrostatic attraction for Ti (Figure 3). This electrostatic force permits Ti to become the center of attraction of the silica framework, as a result of the difference in electronegativity between Ti, Si, and O (1.5; 1.8; 3.5, respectively). Ti–O–Si interaction is believed to be the source of primary elongation since the

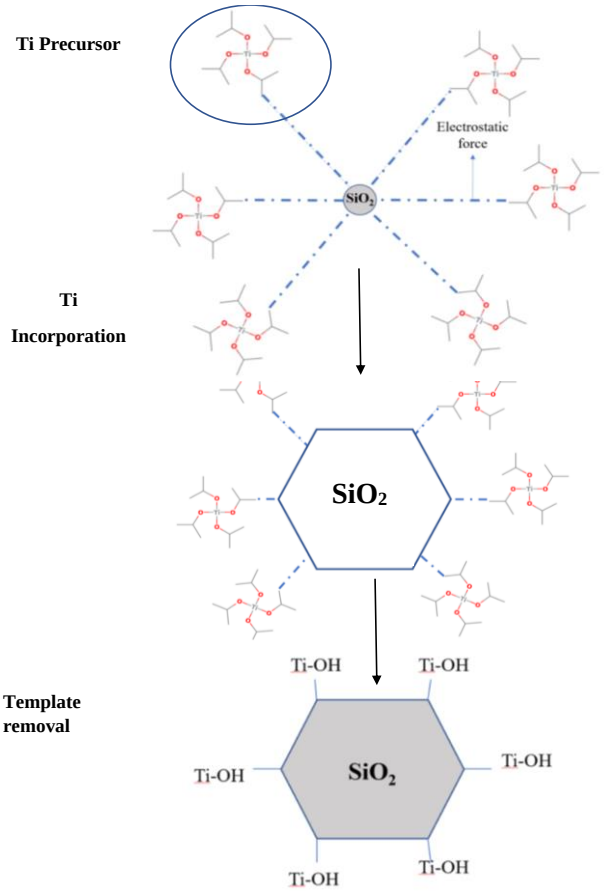

Figure 3. Transformation scheme from microsphere SiO_2 to hexagonal TiO_2/SiO_2 microplates.

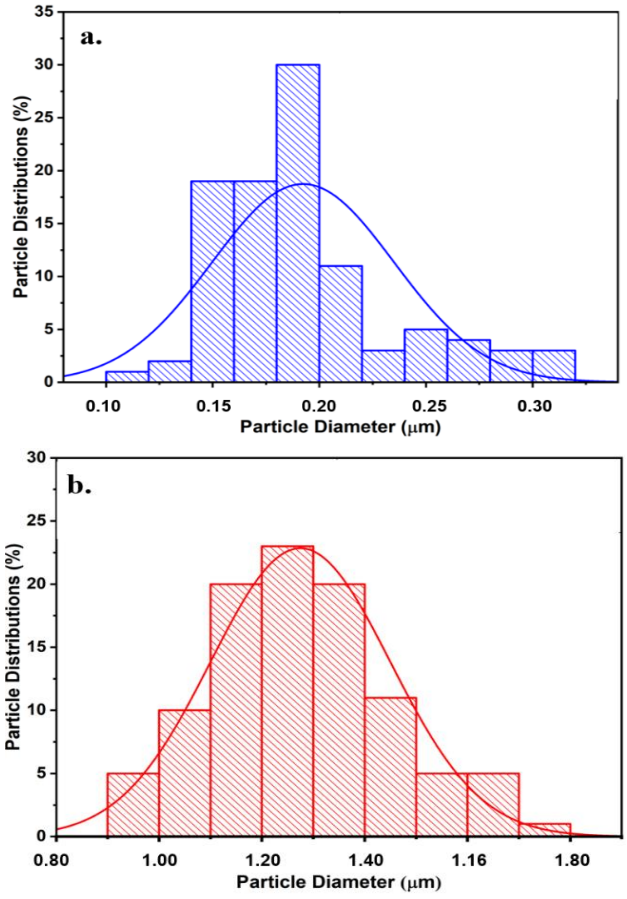

Figure 4. Distribution particle of a. SiO_2 microspheres b. hexagonal TiO_2/SiO_2 porous microplates.

difference in electronegativity between Ti–O and Si–O is around 2.0 and 1.7 then 16 h of constant electrostatic attraction between Ti and silica is what triggers the expansion of the Si framework. As a result, there are changes in the size and shape of silica, particularly the tetragonal anatase, based on the original characteristics of titanium. After organic compund removal from TEOT as Ti precursor, interaction with Ti and Si produces hexagonal plate particles measuring 1.21 µm with TiO_2 scattered over the surface of Silica. Figure 4 indicates that the particle size distribution appears to increase significantly with the addition of TiO_2, indicating that TiO_2 improves the quality of uniformity of silica particles in general, while simultaneously increasing the particle size by up to 84% with the shape transformation from microspheres to hexagonal microplates. XRD confirms that the addition of 0.42% Ti to SiO_2 enhances the crystallinity from 64% to 67% (Table 1). The 15% decrease in Si due to the absorption of fresh Ti and O into the framework demonstrates the success of the incorporation process, which must be evaluated in terms of porosity.

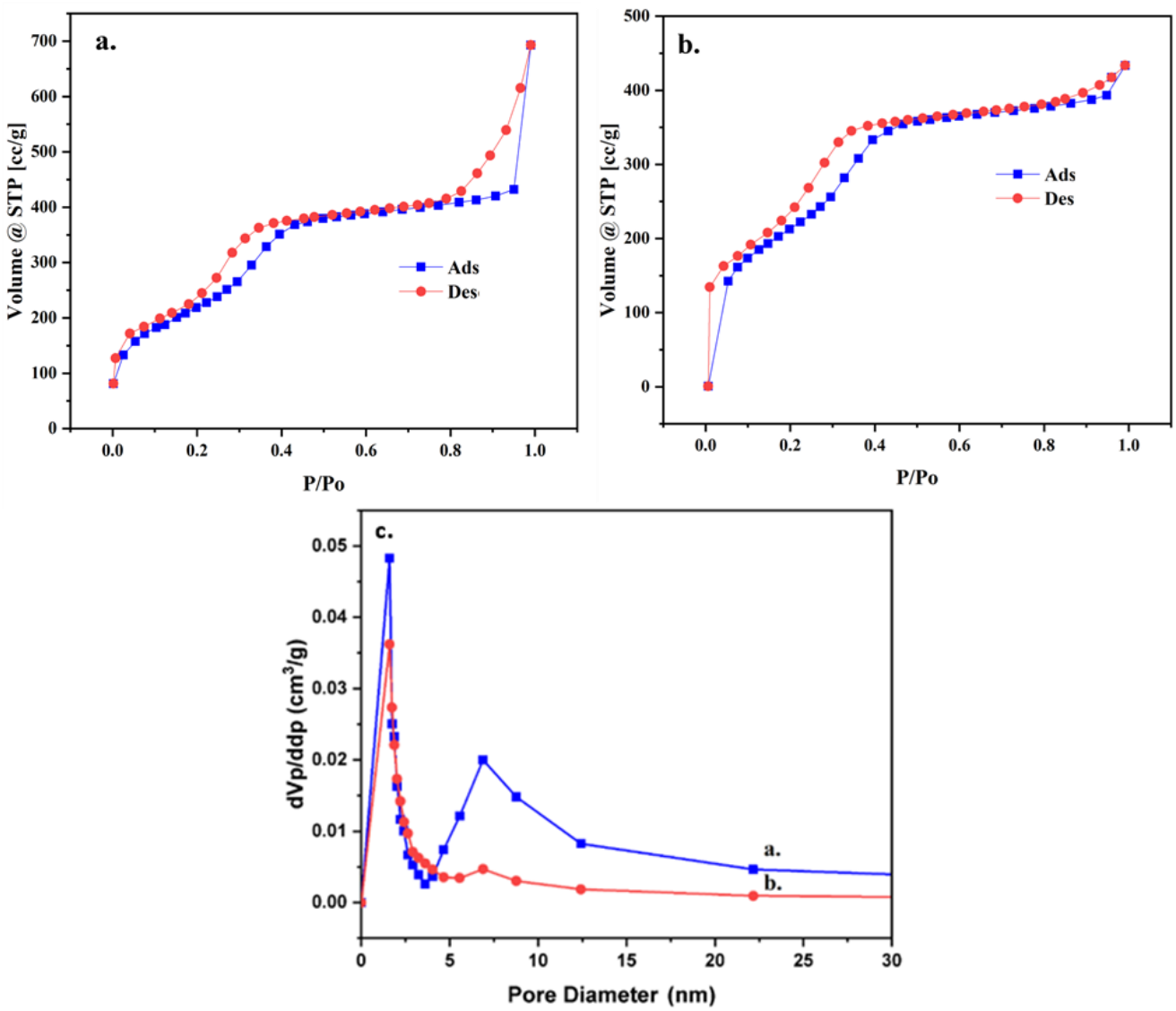

Figure 5. Isotherm adsorption of (a) microsphere SiO_2, (b) hexagonal TiO_2/SiO_2 microplates and (c) Pore size distribution of (a). microsphere SiO_2 and (b). hexagonal TiO_2/SiO_2 microplates

Table 1. Physicochemical properties of samples.

Sample	C[a] (%)	CS[a] (nm)	Element weight[b] (%)				S_{BET}[c] (m^2/g)	V_{total}[d] (cm^3/g)	D[e] (nm)	S_{meso}[f] (m^2/g)	V_{micro}[g] (cm^3/g)	V_{meso}[h] (cm^3/g)
			C	O	Si	Ti						
SM	63.39	0.57	8.46	45.99	45.55	-	809.509	1.023	2.99	707.491	0.5391	0.4839
HTSMP	66.82	0.49	9.06	53.48	37.04	0.42	735.874	0.6707	3.23	268.126	0.3567	0.314

[a]C= Relative crystallinity and CS= crystallite size from XRD results; [b]Element weight by SEM-EDX; [c]S_{BET}= Surface area; [d]V_{total}= Total pore volume; [e]S_{meso}= Surfaces of mesoporous from BJH results; [f]V_{micro}= Micropore volume; [g]V_{meso}= Mesoporous volume.

Figure 5 depicts the isotherms of all samples, which are predominantly type IV with a prominent hysteresis loop, indicating that the material is mesoporous [32]. Table 1 displays the related pore structure parameters, which include specific surface area (S_{BET}), total pore volume (Vt), mesopore surface area and average pore diameter, mesopore volume, and micropore volume. Capillary condensation in uniform pores is characterized by a sharp inflection of SiO_2 microsphere isotherms in the P/P_0 range of 0.3 to 0.7. Due to its huge homogeneous mesopores and narrow pore size distribution (PSD) centered on 2.92 nm, this mesoporous silica has a steep nitrogen absorption at relatively high P/P_0 (Figure 6). Hysteresis loop of Hexagonal TiO_2/SiO_2 Microplates subjected to a greater pressure than SiO_2 microspheres exhibited a larger sample pore size than before TiO_2 incorporation. This is likely owing to the creation of relatively large new pores in the sample after integration because of particle overlapping between TiO_2 and the silica surface or between TiO_2 and silica [33]. Table 1 demonstrates the change in surface area resulting from the transformation of SiO_2 microspheres to hexagonal microplates made of TiO_2/SiO_2 due to the pore blocking effect of TiO_2 particles on the SiO_2 surface, the specific surface area, total pore volume, mesopore surface area, and mesopore volume fell by 8-9%. Due to the creation of new gaps between stacked TiO_2 particles on the SiO_2 surface, the pore width increased by 7% from 2.9 nm to 3.23 nm.

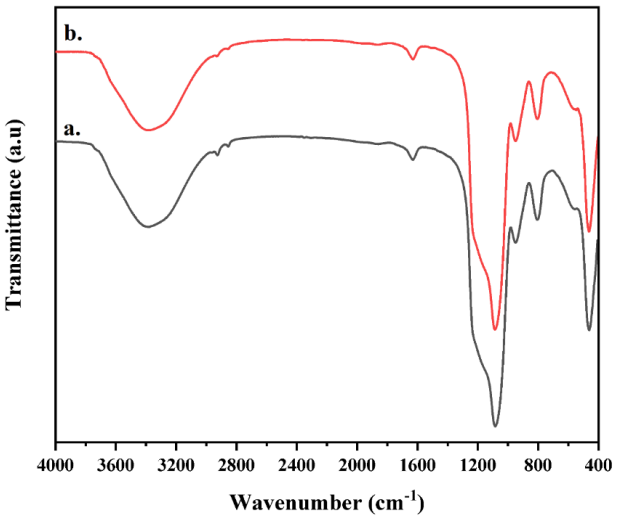

Figure 6. FTIR analysis of (a). microsphere SiO_2, (b). hexagonal TiO_2/SiO_2 microplates.

Examining the FTIR spectra of microsphere SiO_2 and hexagonal TiO_2/SiO_2 microplates is depicted in Figure 6. Broad bands at 3400 cm^{-1} and 1600 cm^{-1} in both spectra are attributable to the stretching and bending vibrations of hydroxyl groups and water adsorbed on the SiO_2 surface [34]. TiO_2/SiO_2 samples exhibit characteristic peaks at 500 cm^{-1}, 1100 cm^{-1}, and 930 cm^{-1}, which correspond to the stretching vibrations of Ti–O, Si–O–Si, and Ti–O–Si, respectively [35]. The spectrum around 820–850 cm^{-1} is characteristic of Si–O–Si and is displayed by both substances [36]. Vibration appears to be a sign of molecular-level Ti–Si interaction.

Figures 7-8 exhibit the photodegradation of methylene blue using TiO_2 as the photoactive material and SiO_2 as the supporting material. When a photon strikes a photoactive semiconductor material, the valence band electrons will be excited into the conduction band. The presence of dark adsorption contributes to homogenization and achieving equilibrium between methylene blue when interacting on the surface of the material, allowing the formation of radicals during UV irradiation to occur more rapidly in the system and resulting in the oxidation of organic compounds occurring more

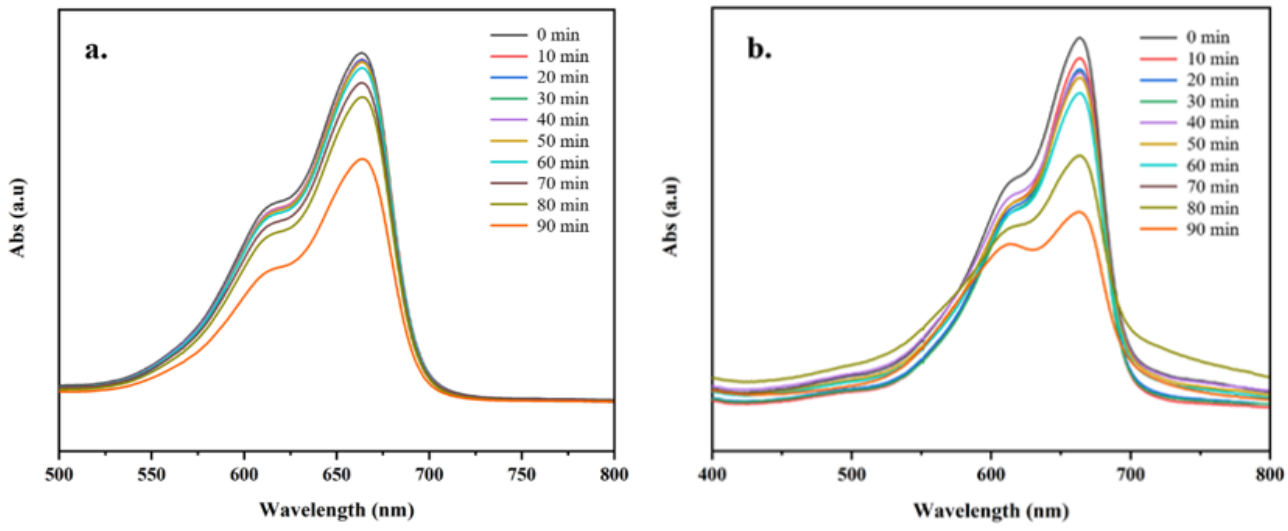

Figure 7. UV-Vis spectra of treated MB solution by photocatalytic degradation of (a). microsphere SiO_2, (b). hexagonal TiO_2/SiO_2 microplates.

rapidly. 5 mg/L of methylene blue was photodegraded by adding 50 mg of catalyst to 200 mL of methylene blue solution that was placed in a solution chamber with a 20 W UV lamp as the photon source. Prior to light irradiation, the suspension was magnetically agitated for 30 min to establish an equilibrium between adsorption and desorption. At a predetermined time, samples were taken, and the treated solution was evaluated using the spectrophotometric method. The pattern of color changes following the photocatalytic breakdown of methylene blue is depicted in Figure 8. It was determined that the presence of all elements contributed to the decolorization of methylene blue and significantly changed the concentration of methylene blue. The sample after impregnation contains silica, titania and oxygen which have different roles because silica with a large surface area increases the homogenization process of methylene blue on the silica surface during the dark adsorption process while titania acts as an active center for photodegradation. The band gap of TiO_2 in subsequent studies is approximately 3.3 eV [37] and changed after incorporation in SiO_2 to 3.21 eV [38], which is the material for confirming the cause of faster degradation in the presence of UV light compared to the material without a photocatalyst under UV light irradiation, which indicates that the SiO_2 material without TiO_2 only adsorbs methylene blue [39]. Initial rate estimates demonstrated that the first 30 min of

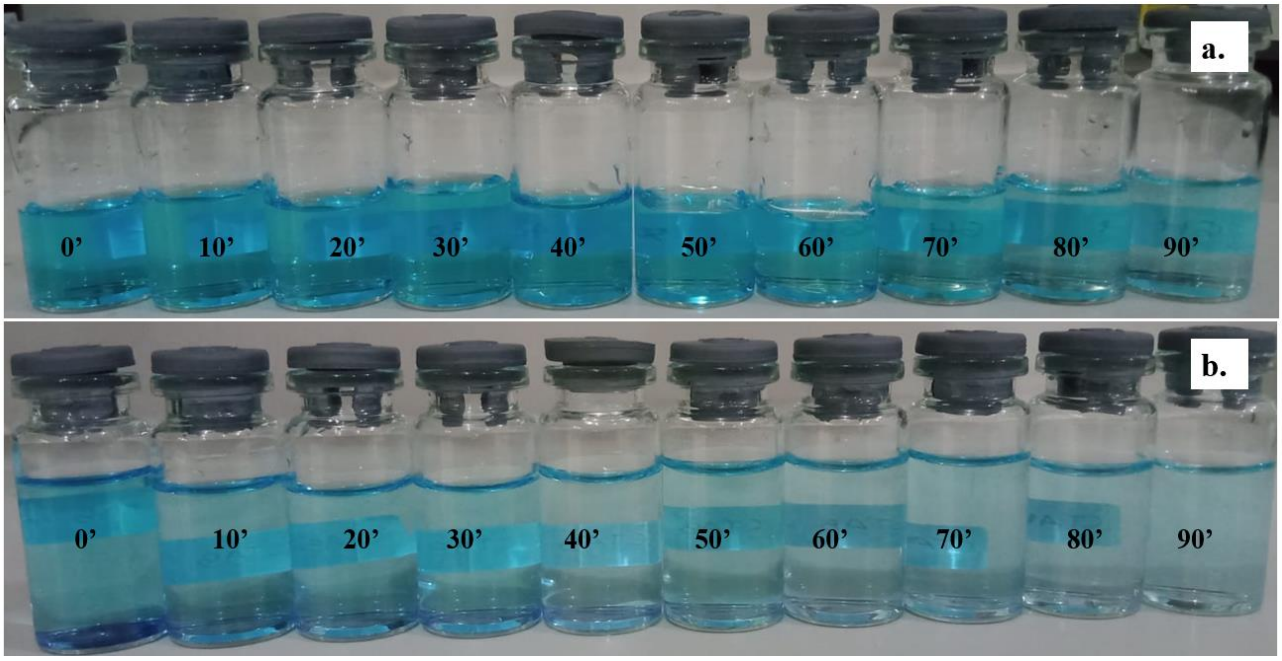

Figure 8. The color change of methylene blue solution at different time of (a). microsphere SiO_2, (b). hexagonal TiO_2/SiO_2 microplates.

Table 2. Photocatalyst for methylene blue degradation.

Catalyst	Dyes Concentration (ppm)	Weight of catalyst (mg)	Ratio of dye concentration : catalyst weight	Time (min)	Catalytic photodegradation (%)	Ref.
CuO nanoparticles	10	50	1:5	105	11.62	[41]
	50	50	1:1	105	80.67	
TiO_2/Pd nanoparticles/ NaY-zeolite	10	50	1:5	120	98.12	[42]
Mn-TiO_2-NPs	10	100	1:10	100	80.00	[43]
Nb_2O_5@PAN/PVDF/ANO	10	150	1:15	240	90	[44]
Ag/TiO_2 nano composite	10	50	1:5	120	96.76	[45]
SiO_2	20	10	2:1	480	45.8	[46]
TiO_2	20	10	2:1	480	30.0	
SiO_2@TiO_2 calcined	20	10	2:1	480	77.8	
TiO_2/SiO_2 Porous Microplates	10	50	1:5	60	81.17	This study

dark adsorption doubled the rate of degradation relative to the absence of dark adsorption. Significantly faster degradation of methylene blue when SiO_2 contains Ti relates to faster radical production accompanied by higher interactions between methylene blue and holes. Under the photooxidation process, all TiO_2/SiO_2 photocatalyst samples degraded around 81% of methylene blue in approximately 60 min (Figure 9). It is also assumed that the total decolorization of methylne blue comes from the presence of Ti as a photocatalyst and Si as a supporting material which functions to disperse the catalyst. The greater the surface area of silica as a supporting material, the better the Ti dispersion will be. Ti on the silica surface has band gap energy, resulting in higher decolorization compared to silica alone because the homogenization process during dark adsorption and photodegradation takes place optimally. Another assumption is that silica only decolorizes with an adsorption step starting from the first step in dark conditions until the next step in the last 90 min [40]. This study was compared with other studies (Table 2) and proved that the degradation was more than other catalyst (under 60 min).

4. Conclusion

The integration of a Ti precursor into SiO_2 generated by the hydrothermal technique in a gelatin-CTAB template led to the effective synthesis of a highly efficient TiO_2/SiO_2 photocatalyst. The findings of the analysis indicate that the product consists of hexagonal TiO_2/SiO_2 porous microplates with a crystallinity of approximately 67%, a surface area of 735 m^2/g, a pore volume of 0.67 cm^3/g, and a pore diameter of 3.2 nm. Hexagonal TiO_2/SiO_2 porous microplates as a photocatalyst with photocatalytic efficiency of 81% under UV light irradiation with a 30 min dark adsorption process concludes that this photocatalyst is very likely to be a future photocatalyst candidate due to the high sustainability of the SiO_2 supporting material, which is created using gelatin as a natural template.

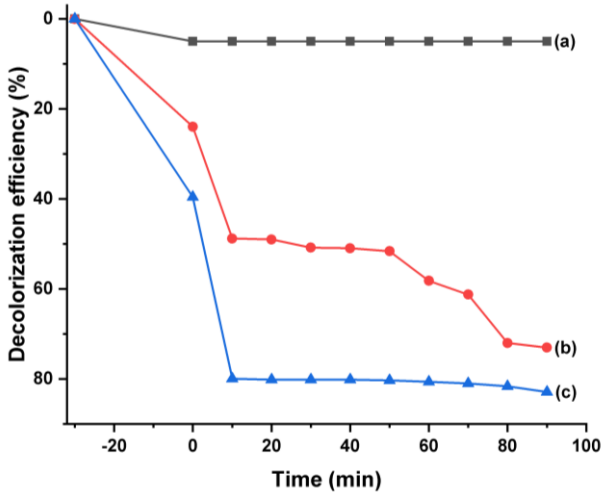

Figure 9. Photocatalytic degradation of (a). no catalyst, (b). microsphere SiO_2, and (c). hexagonal TiO_2/SiO_2 microplates.

Acknowledgements

This research was supported by the Universitas Sebelas Maret on International Collaboration grant 2024 under Maria Ulfa.

CRediT Author Statement

Author Contributions: *M. Ulfa:* Conceptualization, Investigation, Resources, Data Curation, Writing, Review and Editing, Supervision; *C.N. Anggreani*: Methodology, Formal Analysis, Data Curation, Writing Draft Preparation; *B. Mulyani:* Review and Editing, Data Curation; *N.A. Sholeha:* Review and Editing, Data Curation, and Validation. All authors have read and agreed to the published version of the manuscript.

References

[1] Ramutshatsha-makhwedzha, D., Mavhungu, A., Moropeng, M.L., Mbaya, R. (2023). Heliyon Activated carbon derived from waste orange and lemon peels for the adsorption of methyl orange and methylene blue dyes from wastewater. *Heliyon*, 8, e09930. DOI: 10.1016/j.heliyon.2022.e09930.

[2] Radoor, S., Karayil, J., Jayakumar, A., Parameswaranpillai, J., Siengchin, S. (2021). Release of toxic methylene blue from water by mesoporous silicalite-1: characterization, kinetics and isotherm studies. *Applied Water Science*, 11(7), 1–12. DOI: 10.1007/s13201-021-01435-z.

[3] Calzada, L.A., Castellanos, R., García, L.A., Klimova, T.E. (2019). TiO2, SnO2 and ZnO catalysts supported on mesoporous SBA-15 versus unsupported nanopowders in photocatalytic degradation of methylene blue. Microporous and Mesoporous Materials, 285, 247-258. DOI: 10.1016/j.micromeso.2019.05.015.

[4] Tuna, M., Yanalak, G., Arslan, G., Hatay, I. (2020). Materials Science in Semiconductor Processing Green preparation of Carbon Quantum dots using Gingko biloba to sensitize TiO 2 for the photohydrogen production. *Materials Science in Semiconductor Processing*, 109, 104945. DOI: 10.1016/j.mssp.2020.104945.

[5] Lee, S.J., Jung, H.J., Koutavarapu, R., Lee, S.H., Arumugam, M., Kim, J.H., Choi, M.Y. (2019). ZnO supported Au/Pd bimetallic nanocomposites for plasmon improved photocatalytic activity for methylene blue degradation under visible light irradiation. *Applied Surface Science*, 496, 143665. DOI: 10.1016/j.apsusc.2019.143665.

[6] Samadi, M., Zirak, M., Naseri, A., Khorashadizade, E., Moshfegh, A.Z. (2016). Recent progress on doped ZnO nanostructures for visible-light photocatalysis. *Thin Solid Films*, 605, 2–19. DOI: 10.1016/j.tsf.2015.12.064.

[7] Prasetyoko, D., Sholeha, N.A., Subagyo, R., Ulfa, M., Bahruji, H., Holilah, H., Pradipta, M.F., Jalil, A.A. (2023). Mesoporous ZnO nanoparticles using gelatin — Pluronic F127 as a double colloidal system for methylene blue photodegradation. *Korean Journal of Chemical Engineering*, 40 (1), 112–123. DOI: 10.1007/s11814-022-1224-y.

[8] Li, J., Han, L., Zhang, T., Qu, C., Yu, T., Yang, B. (2022). Removal of Methylene Blue by Metal Oxides Supported by Oily Sludge Pyrolysis Residues. *Applied Sciences (Switzerland)*, 12(9), 4725. DOI: 10.3390/app12094725.

[9] Sapkota, K.P., Islam, M.A., Hanif, M.A., Akter, J., Lee, I., Hahn, J.R. (2021). Hierarchical nanocauliflower chemical assembly composed of copper oxide and single-walled carbon nanotubes for enhanced photocatalytic dye degradation. *Nanomaterials*, 11 (3), 696. DOI: 10.3390/nano11030696.

[10] Shin, J., Andreas Hutomo, C., Kim, J., Jang, J., Beum Park, C. (2022). Natural pollen exine-templated synthesis of photocatalytic metal oxides with high surface area and oxygen vacancies. *Applied Surface Science*, 599, 154064. DOI: 10.1016/j.apsusc.2022.154064.

[11] Cheng, Z., Luo, S., Liu, Z., Zhang, Y., Liao, Y., Guo, M., Nguyen, T.T. (2022). Visible-light-driven hierarchical porous CeO_2 derived from wood for effective photocatalytic degradation of methylene blue. *Optical Materials*, 129, 112429. DOI: 10.1016/j.optmat.2022.112429.

[12] Ulfa, M., Al Afif, H., Saraswati, T.E., Bahruji, H. (2022). Fast Removal of Methylene Blue via Adsorption-Photodegradation on TiO_2/SBA-15 Synthesized by Slow Calcination. *Materials*, 15(16), 5471. DOI: 10.3390/ma15165471.

[13] Ulfa, M., Prasetyoko, D., Trisunaryanti, W., Bahruji, H., Fadila, Z.A., Sholeha, N.A. (2022). The effect of gelatin as pore expander in green synthesis mesoporous silica for methylene blue adsorption. *Scientific Reports*, 12(1), 1–12. DOI: 10.1038/s41598-022-19615-5.

[14] Anjum, M., Kumar, R., Abdelbasir, S.M., Barakat, M.A. (2018). Carbon nitride/titania nanotubes composite for photocatalytic degradation of organics in water and sludge: Pre-treatment of sludge, anaerobic digestion and biogas production. *Journal of Environmental Management*, 223, 495–502. DOI: 10.1016/j.jenvman.2018.06.043.

[15] Wang, Y., Lu, Y., Luo, R., Zhang, Y., Guo, Y., Yu, Q. (2018). Densely-stacked N-doped mesoporous TiO_2/carbon microsphere derived from outdated milk as high-performance electrode material for energy storages. *Ceramics International*, 44(14), 16265–16272. DOI: 10.1016/j.ceramint.2018.06.020.

[16] Naseem, S., Khan, W., Khan, S., Uddin, I., Raza, W., Shoeb, M., Mobin, M., Naqvi, A.H. (2019). Enhanced Photocatalytic Activity by Tuning of Structural and Optoelectrical Properties of Cr(III) Incorporated TiO_2 Nanoparticles. *Journal of Electronic Materials*, 48, 7203–7215. DOI: 10.1007/s11664-019-07499-7.

[17] Zheng, X., Zhang, X., Hu, Q., Sun, H., Wang, L., Li, X. (2021). Adsorption and photocatalytic activity of nano-magnetic materials fe3o4@c@tio2-agbr-ag for rhodamine b. *Current Nanoscience*, 17 (3), 484–493. DOI: 10.2174/1573413716999200820144001.

[18] Marfur, N.A., Jaafar, N.F., Khairuddean, M., Nordin, N. (2020). A Review on Recent Progression of Modifications on Titania Morphology and its Photocatalytic Performance. *Acta Chimica Slovenica*, 67(2), 361–374. DOI: 10.17344/acsi.2019.5161.

[19] Herath, A., Navarathna, C., Warren, S., Perez, F., Pittman, C.U., Mlsna, T.E. (2022). Iron/titanium oxide-biochar (Fe_2TiO_5/BC): A versatile adsorbent/photocatalyst for aqueous Cr(VI), Pb^{2+}, F- and methylene blue. *Journal of Colloid and Interface Science*, 614, 603–616. DOI: 10.1016/j.jcis.2022.01.067.

[20] Jin, X., Che, R., Yang, J., Liu, Y., Chen, X., Jiang, Y., Liang, J., Chen, S., Su, H. (2022). Activated Carbon and Carbon Quantum Dots/Titanium Dioxide Composite Based on Waste Rice Noodles: Simultaneous Synthesis and Application in Water Pollution Control. *Nanomaterials*, 12(3), 472. DOI: 10.3390/nano12030472.

[21] Brossault, D.F.F., McCoy, T.M., Routh, A.F. (2021). Self-assembly of TiO_2/Fe_3O_4/SiO_2 microbeads: A green approach to produce magnetic photocatalysts. *Journal of Colloid and Interface Science*, 584, 779–788. DOI: 10.1016/j.jcis.2020.10.001.

[22] Wei, J., Wen, X., Zhu, F. (2018). Influence of Surfactant on the Morphology and Photocatalytic Activity of Anatase TiO_2 by Solvothermal Synthesis. *Journal of Nanomaterials*, 2018, 3086269. DOI: 10.1155/2018/3086269.

[23] Sanad, M.M.S., Farahat, M.M., El-Hout, S.I., El-Sheikh, S.M. (2021). Preparation and characterization of magnetic photocatalyst from the banded iron formation for effective photodegradation of methylene blue under UV and visible illumination. *Journal of Environmental Chemical Engineering*, 9(2), 105127. DOI: 10.1016/j.jece.2021.105127.

[24] Coradin, T., Bah, S., Livage, J. (2004). Gelatine/silicate interactions: From nanoparticles to composite gels. *Colloids and Surfaces B: Biointerfaces*, 35 (1), 53–58. DOI: 10.1016/j.colsurfb.2004.02.008.

[25] El-Hakam, S.A., ALShorifi, F.T., Salama, R.S., Gamal, S., El-Yazeed, W.S.A., Ibrahim, A.A., Ahmed, A.I. (2022). Application of nanostructured mesoporous silica/ bismuth vanadate composite catalysts for the degradation of methylene blue and brilliant green. *Journal of Materials Research and Technology*, 18, 1963–1976. DOI: 10.1016/j.jmrt.2022.03.067.

[26] Ulfa, M., Nur, C., Amalia, N. (2023). Fine-tuning mesoporous silica properties by a dual-template ratio as TiO_2 support for dye photodegradation booster. *Heliyon*, 9(6), e16275. DOI: 10.1016/j.heliyon.2023.e16275.

[27] Khairy, M., Zakaria, W. (2014). Effect of metal-doping of TiO_2 nanoparticles on their photocatalytic activities toward removal of organic dyes. *Egyptian Journal of Petroleum*, 23(4), 419–426. DOI: 10.1016/j.ejpe.2014.09.010.

[28] Fujimoto, K., Watanabe, K., Ishikawa, S., Ishii, H., Suga, K. (2021). Pore expanding effect of hydrophobic agent on 100 nm-sized mesoporous silica particles estimated based on Hansen solubility parameters. *Colloids and Surfaces A*, 609, 125647. DOI: 10.1016/j.colsurfa.2020.125647.

[29] Chanhom, P., Charoenlap, N., Tomapatanaget, B., Insin, N. (2017). Colloidal titania-silica-iron oxide nanocomposites and the effect from silica thickness on the photocatalytic and bactericidal activities. *Journal of Magnetism and Magnetic Materials*, 427, 54–59. DOI: 10.1016/j.jmmm.2016.10.123.

[30] Fatimah, I., Prakoso, N.I., Sahroni, I., Musawwa, M.M., Sim, Y.L., Kooli, F., Muraza, O. (2019). Physicochemical characteristics and photocatalytic performance of TiO_2/SiO_2 catalyst synthesized using biogenic silica from bamboo leaves. *Heliyon*, 5 (11), e02766. DOI: 10.1016/j.heliyon.2019.e02766.

[31] Nguyen, Q.N.K., Yen, N.T., Hau, N.D., Tran, H.L. (2020). Synthesis and Characterization of Mesoporous Silica SBA-15 and ZnO/SBA-15 Photocatalytic Materials from the Ash of Brickyards. *Journal of Chemistry*, 2020, 8456194. DOI: 10.1155/2020/8456194.

[32] Kibona, T.E. (2020). Synthesis of NiCo2O4/mesoporous carbon composites for supercapacitor electrodes. *Journal of Solid State Electrochemistry*, 24(7), 1587–1598. DOI: 10.1007/s10008-020-04673-4.

[33] Abdolahi Sadatlu, M.A., Mozaffari, N. (2016). Synthesis of mesoporous TiO_2 structures through P123 copolymer as the structural directing agent and assessment of their performance in dye-sensitized solar cells. Solar Energy, 24–34. DOI: 10.1016/j.solener.2016.03.056.

[34] de Souza, C.C., de Souza, L.Z.M., Yılmaz, M., de Oliveira, M.A., da Silva Bezerra, A.C., da Silva, E.F., Dumont, M.R., Machado, A.R.T. (2022). Activated carbon of Coriandrum sativum for adsorption of methylene blue: Equilibrium and kinetic modeling. *Cleaner Materials*, 3, 100052. DOI: 10.1016/j.clema.2022.100052.

[35] Sharma, R.K., Wang, S., Maity, J.P., Banerjee, P., Dey, G., Huang, Y., Bundschuh, J., Hsiao, P., Chen, T., Chen, C. (2021). A novel BMSN (biologically synthesized mesoporous silica nanoparticles) material: synthesis using a bacteria-mediated biosurfactant and characterization. *RSC Advances*, 11, 32906. DOI: 10.1039/d1ra05852e.

[36] Usgodaarachchi, L., Thambiliyagodage, C., Wijesekera, R., Bakker, M.G. (2021). Synthesis of mesoporous silica nanoparticles derived from rice husk and surface-controlled amine functionalization for efficient adsorption of methylene blue from aqueous solution. *Current Research in Green and Sustainable Chemistry*, 4, 100116. DOI: 10.1016/j.crgsc.2021.100116.

[37] Bet-Moushoul, E., Mansourpanah, Y., Farhadi, K., Tabatabaei, M. (2016). TiO_2 nanocomposite based polymeric membranes: A review on performance improvement for various applications in chemical engineering processes. *Chemical Engineering Journal*, 283, 29–46. DOI: 10.1016/j.cej.2015.06.124.

[38] Fatimah, I., Iman, N., Sahroni, I., Musawwa, M.M. (2019). Physicochemical characteristics and photocatalytic performance of TiO_2/SiO_2 catalyst synthesized using biogenic silica from bamboo leaves. *Heliyon*, 5, e02766. DOI: 10.1016/j.heliyon.2019.e02766.

[39] Lin, T.H., Thang, T.Q., An, H., Hai, N.D. (2023). Synthesis of TiO_2-doped carbon aerogel from sugarcane bagasse for high efficiency of photodegradation of methylene blue in the water. *Vietnam Journal Chemistry*, 61(2), 227–237. DOI: 10.1002/vjch.202200128.

[40] Li, W., Liang, R., Zhou, N.Y., Pan, Z. (2020). Carbon Black-Doped Anatase TiO_2 Nanorods for Solar Light-Induced Photocatalytic Degradation of Methylene Blue. *ACS Omega*, 5, 10042−10051. DOI: 10.1021/acsomega.0c00504.

[41] Nouren, S., Bibi, I., Kausar, A., Sultan, M., Nawaz, H., Safa, Y., Sadaf, S., Alwadai, N., Iqbal, M. (2024). Green synthesis of CuO nanoparticles using Jasmin sambac extract: Conditions optimization and photocatalytic degradation of Methylene Blue dye. *Journal of King Saud University - Science*, 36, 103089. DOI: 10.1016/j.jksus.2024.103089.

[42] Bello, M.O., Prabhakar, S., Abdus-salam, N., Adekola, F.A., Shobha, C., Sesha, A. V, Pal, U. (2024). Na-Y zeolite supported TiO_2/Pd nanoparticles for enhanced photoredox catalytic properties and green hydrogen generation. *Catalysis Communications*, 186, 106817. DOI: 10.1016/j.catcom.2023.106817.

[43] Awan, A.M., Khalid, A., Ahmad, P., Alharthi, A.I., Farooq, M., Khan, A., Khandaker, M.U., Aldawood, S., Alotaibi, M.A., El-Mansi, A.A., Eldesoqui, M.B., Dawood, A.F., Zyoud, S.H. (2024). Defects oriented hydrothermal synthesis of TiO_2 and $MnTiO_2$ nanoparticles as photocatalysts for wastewater treatment and antibacterial applications. *Heliyon*, 10, e25579. DOI: 10.1016/j.heliyon.2024.e25579.

[44] Rianjanu, A., Deny, K., Marpaung, P., Kartini, E., Melati, A., Rizky, A., Gusti, Y., Mahendra, I.P., Yulianto, N., Widakdo, J., Triyana, K., Suryo, H., Taher, T. (2023). Integrated adsorption and photocatalytic removal of methylene blue dye from aqueous solution by hierarchical Nb_2O_5@PAN/PVDF/ANO composite nano fibers. *Nano Materials Science*, in press. DOI: 10.1016/j.nanoms.2023.10.006

[45] Septiningrum, F., Herman, A., Akbar, F. (2024). Mangosteen pericarp extract mediated synthesis of Ag/TiO_2 nanocomposite and its application on organic pollutant degradation by adsorption-photocatalytic activity. *Current Research in Green and Sustainable Chemistry*, 8, 100394. DOI: 10.1016/j.crgsc.2023.100394.

[46] Gomes, B.R., Lopes, J.L., Coelho, L., Ligonzo, M., Rigoletto, M., Magnacca, G., Deganello, F. (2023). Development and Upscaling of SiO_2@TiO_2 Core-Shell Nanoparticles for Methylene Blue Removal. *Nanomaterials*, 13(16), 2276. DOI: 10.3390/nano13162276.